Article

Chinese Science Bulletin

Atmospheric Science

April 2012 Vol.57 No.10: 1188–1195
doi: 10.1007/s11434-011-4935-8

Climate change in China in the 21st century as simulated by a high resolution regional climate model

GAO XueJie[1*], SHI Ying[1], ZHANG DongFeng[2] & GIORGI Filippo[3]

[1] *National Climate Center, China Meteorological Administration, Beijing 100081, China;*
[2] *Shanxi Climate Center, Taiyuan 030006, China;*
[3] *The Abdus Salam International Centre for Theoretical Physics, Trieste 34100, Italy*

Received September 30, 2011; accepted December 5, 2011; published online February 7, 2012

Climate change in the 21st century over China is simulated using the Abdus Salam International Centre for Theoretical Physics (ICTP) Regional Climate Model version 3 (RegCM3). The model is one-way nested within the global model CCSR/NIES/FRCGC MIROC3.2_hires (Center for Climate System Research/National Institute for Environmental Studies/Frontier Research Center for Global Change/Model for Interdisciplinary Research on Climate). A 150-year (1951–2100) transient simulation is conducted at 25 km grid spacing, under the Intergovernmental Panel on Climate Change Special Report on Emissions Scenarios (IPCC SRES) A1B scenario. Simulations of present climate conditions in China by RegCM3 are compared against observations to assess model performance. Results show that RegCM3 reproduces the observed spatial structure of surface air temperature and precipitation well. Changes in mean temperature and precipitation in December-January-February (DJF) and June-July-August (JJA) during the middle and end of the 21st century are analyzed. Significant future warming is simulated by RegCM3. This warming becomes greater with time, and increased warming is simulated at high latitude and high altitude (Tibetan Plateau) areas. In the middle of the 21st century in DJF, a general increase of precipitation is found in most areas, except over the Tibetan Plateau. Precipitation changes in JJA show an increase over northwest China and a decrease over the Tibetan Plateau. There is a mixture of positive and negative changes in eastern China. The change pattern at the end of the century is generally consistent with that in mid century, except in some small areas, and the magnitude of change is usually larger. In addition, the simulation is compared with a previous simulation of the RegCM3 driven by a different global model, to address uncertainties of the projected climate change in China.

climate change, regional climate model, China, numerical simulation, uncertainty

Citation: Gao X J, Shi Y, Zhang D F, et al. Climate change in China in the 21st century as simulated by a high resolution regional climate model. Chin Sci Bull, 2012, 57: 1188–1195, doi: 10.1007/s11434-011-4935-8

Significant warming has been observed globally, which is very likely because of the increase in anthropogenic concentration of greenhouse gases. By the end of the 21st century (2090–2099), the likely range of global temperature increase is projected to be 1.1–6.4°C (relative to 1980–1999) [1].

While atmosphere-ocean coupled general circulation models (AOGCMs) are the primary tools for climate change projections, they have deficiencies at the regional and local scale because of their coarse resolutions. High-resolution regional climate models (RCMs) have been developed [2] and are now widely used to downscale AOGCM information [3]. High-resolution climate scenarios are also important in satisfying a great demand from impact assessment studies at the regional and local scale.

High-resolution RCMs usually project different change patterns of precipitation compared to the driving general circulation model (GCM), because of their much stronger and more realistic topographic forcings [4–6]. Use of RCMs is particularly important for East Asia, because of its complex topography and unique weather and climate systems [3,5,7–13].

We present results from a continuous climate change experiment for the period 1951–2100 at 25 km grid spacing over China, generated by an RCM (RegCM3; see below).

*Corresponding author (email: gaoxj@cma.gov.cn)

The analysis is focused on mean temperature and precipitation in December-January-February (DJF) and June-July-August (JJA).

1 Model and experimental design

The RCM used in the present work is the Abdus Salam International Centre for Theoretical Physics (ICTP) Regional Climate Model version 3 (RegCM3), which is based on the model of Giorgi et al. [14,15] and includes upgrades described by Pal et al. [16]. The horizontal grid spacing of RegCM3 is 25 km, and the model domain covers all of China and surrounding East Asia areas (Figure 1). The model has a standard vertical configuration of 18 sigma layers, with model top at 10 hPa. Atmospheric radiation transfer in the model is computed using the radiation package from the National Center for Atmospheric Research Community Climate Model (NCAR CCM3) [17], the ocean flux parameterization follows Zeng et al. [18], and the planetary boundary layer computations use the non-local formulation of Holtslag et al. [19]. Resolvable-scale precipitation is represented by the scheme of Pal et al. [20], and convective precipitation by the mass flux scheme of Grell [21] based on the Fritsch-Chappell closure assumption [22]. Surface processes are executed with the Biosphere-Atmosphere Transfer Scheme (BATS) [23].

Model vegetation cover is obtained from the observed data of Liu et al. [24] within China, and from the satellite-based Global Land Cover Characterization (GLCC) database outside China. Initial and time evolving lateral boundary conditions at 6-hour intervals for temperature, surface pressure, wind (meridional and zonal components) and specific humidity are provided by CCSR/NIES/FRCGC MIROC3.2_hires simulations [25], under the IPCC SRES A1B scenario (the former acronyms are for Center for Climate System Research/National Institute for Environmental Studies/Frontier Research Center for Global Change/Model for Interdisciplinary Research on Climate; the latter are Intergovernmental Panel on Climate Change Special Report on Emissions Scenarios). Horizontal resolution of the atmospheric component of MIROC3.2_hires is T106 (~125 km). As the model with the highest spatial resolution in the Coupled Model Intercomparison Project (CMIP3) archive, MIROC3.2_hires shows good performance in simulating present climate, particularly over East Asia [26,27].

The period of climate change simulation of RegCM3 is from 1948 to 2100, for a total of 153 years. The first three years are used for model spin-up, and are thus not included in the analysis. The period 1981–2000 is considered present day, and 2001–2100 is the future. The term "change" refers to the difference between the latter and former periods in the simulation. To the authors' knowledge, this is the first time that such a high-resolution RCM has been run consecutively over this long period and domain.

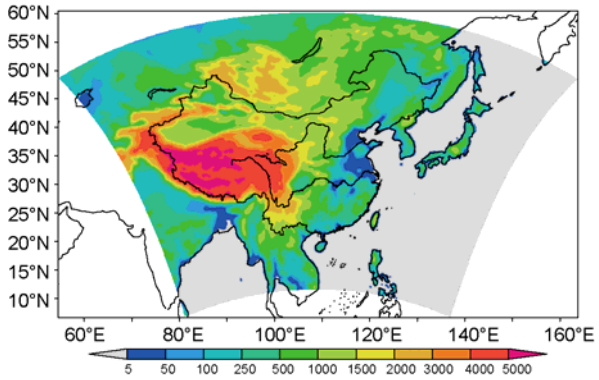

Figure 1 Model domain and topography (m).

To validate model performance, we used the observation dataset of surface air temperature developed by Xu et al. [28] (CN05), and of precipitation by Xie et al. [29] (Xie). Both datasets have a 0.5° latitude by 0.5° longitude resolution. To facilitate the analysis, model output and the observation dataset are interpolated to a common 0.25° latitude by 0.25° longitude grid.

2 Validation of present day simulation

2.1 Surface air temperature

The simulation of mean temperature for present day (1981–2000) by RegCM3 is first compared with observations. As shown in Figure 2(a) and (c), both the spatial distribution and magnitude of observed temperature are well reproduced by the model in DJF. The model also captures spatial details, such as the high values in the Junggar, Qaidam and Sichuan basins, and low values in the Tianshan and Qilianshan mountains. Differences between the model simulation and observations are usually within 1°C, except for a large warm bias of a few degrees in Northeast and Northwest China, and a general cold bias over the Tibetan Plateau. The warm bias at high latitude in the cold season is a typical model deficiency of RegCM3, even when driven by reanalysis [30].

Similarly, the model reproduces the main features of temperature patterns and values in JJA. Biases are found in North China and the deserts of the Northwest (warm bias of 1–3°C), on the Tibetan Plateau and in the southern extreme of China (cold bias of 1–2°C). The spatial correlation coefficient between model simulation and observation is 0.95 and 0.98 in DJF and JJA, respectively.

2.2 Precipitation

Figure 3 shows the distribution of observed and simulated precipitation in DJF and JJA. In DJF, observed precipitation maxima with values greater than 250 mm are located in southeastern areas. The precipitation decreases toward the north and west (Figure 3(a)). In the RegCM3 simulation

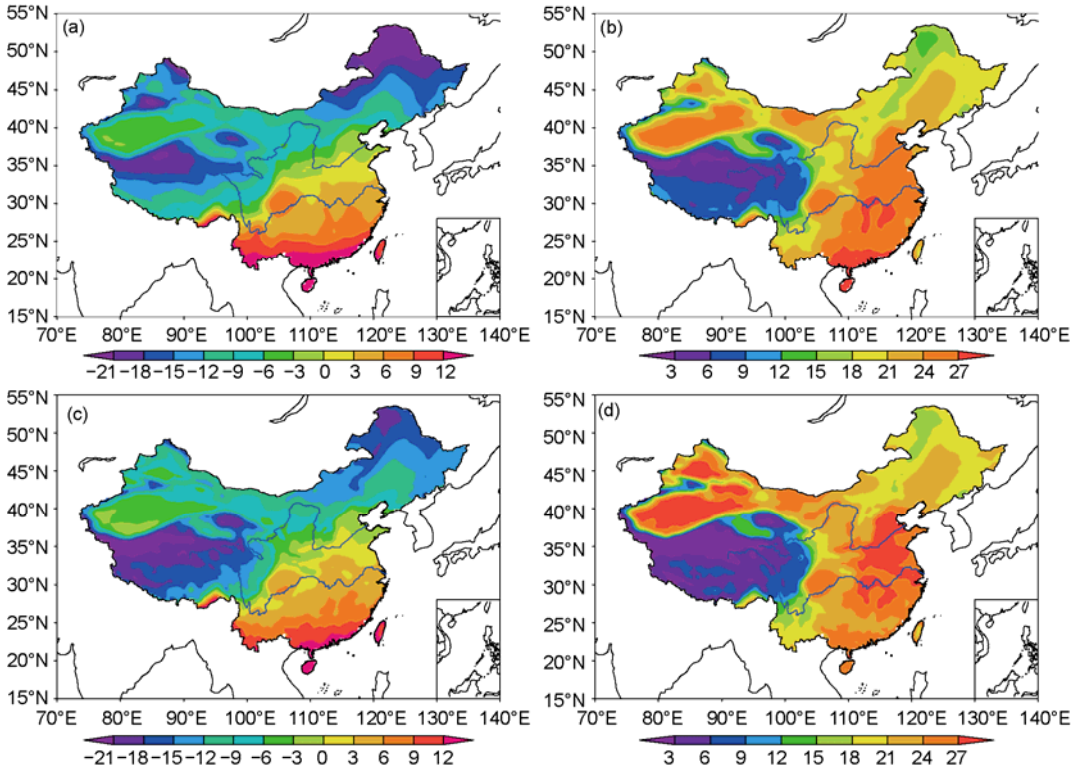

Figure 2 Mean temperature in DJF and JJA over China (1981–2000) (°C). (a) Observation in DJF; (b) observation in JJA; (c) simulation in DJF by RegCM3; (d) simulation in JJA by RegCM3.

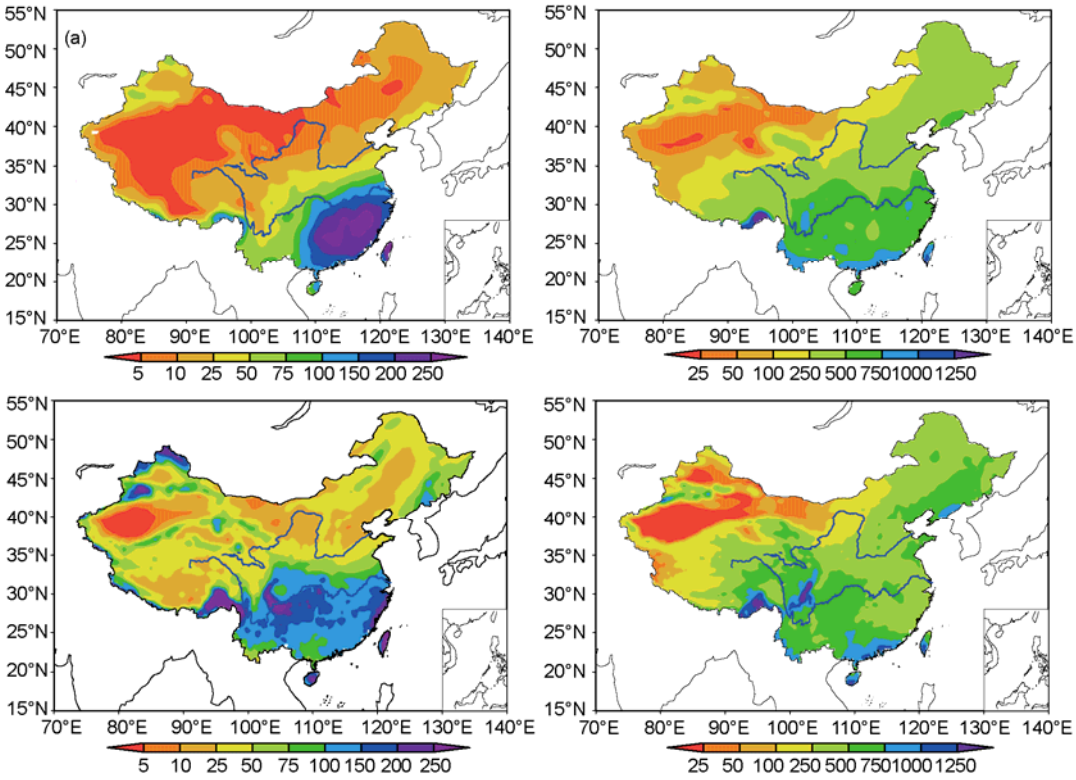

Figure 3 Same as in Figure 2, but for precipitation (mm).

(Figure 3(c)), there is an overall pattern of a wetter south, and a drier north and northwest. However, the amount of precipitation in South China is underestimated, and two small-scale precipitation centers in the western and eastern parts of Southern China are simulated, instead of the one maximum from the observation. The model also overestimates precipitation in North China. Similar model discrepancies are evidenced when driven by reanalysis and a different GCM [30,31]. The spatial correlation coefficient between model simulation and observation is 0.58 in DJF.

A higher correlation coefficient (0.82) between model simulation and observation is found in JJA. This improved seasonal performance is evident when comparing Figure 3(d) with (b). The model simulation agrees well with observation, in both spatial distribution and amount, except for underestimation on the southeast coast and overestimation in eastern sections of the Northeast. The model reproduces well the topographically induced precipitation patterns in the Northwest, e.g. the larger values over Tianshan Mountain and smaller values in the two basins to its north and south.

3 Future changes

3.1 Surface air temperature

Figure 4 shows distributions of temperature change in DJF and JJA for the middle (2041–2060) and end (2081–2100) of the 21st century, from the RegCM3 simulation. Substantial warming is found in both seasons and periods. The warming is more pronounced at the end of the century, compared to the middle.

In the middle of the 21st century in DJF, greater warming is found in northern areas and over the Tibetan Plateau, compared to the south (Figure 4(a)). The warming is least (less than 2.4°C) in Southwest China, and greatest (exceeding 4.2°C) in the southern Tibetan Plateau. The pattern of warming is similar at the end of the century in DJF compared to the middle, but with larger values. The minimum and maximum warming are also found in the Southwest and Tibetan Plateau, with values less than 4.2°C and greater than 7°C, respectively. Simulated increases in temperature elsewhere are between 4.5°C and 6.5°C (Figure 4(b)). Regional mean temperature changes in the middle and end of the century in DJF are 3.1°C and 5.5°C, respectively.

In JJA, maximum warming greater than 4.2°C is found in areas extending from North China to most of the Northeast. Less than 2.4°C warming is simulated in South China. Warming over the Tibetan Plateau is within a medium range, between 2.7°C and 3.3°C (Figure 4(c)). As in DJF, the warming pattern in JJA at the end of the century is similar to the middle, but has a much larger extent. For example, the warming in the central Northeast is as much as 7°C (Figure 4(d)). Regional mean temperature changes in the middle and end of the 21st century in JJA are 3.0°C and

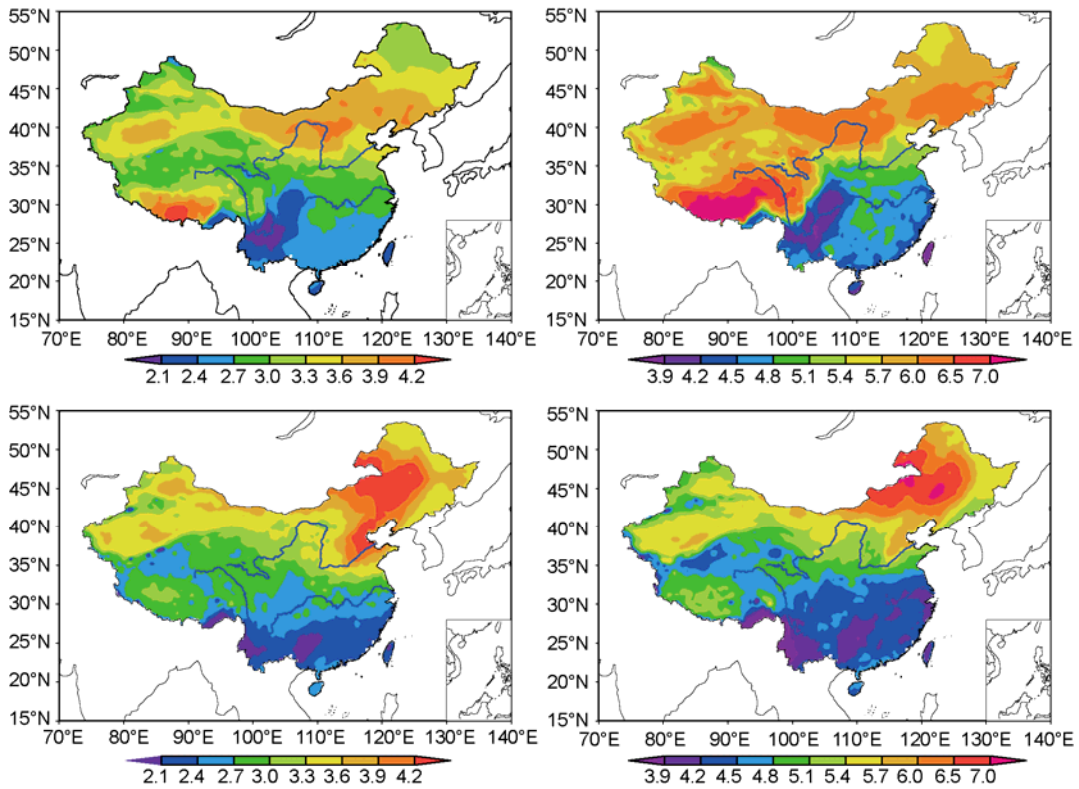

Figure 4 Changes of temperature over China simulated by RegCM3 (°C). (a) DJF in middle of the 21st century (2041–2060); (b) DJF at the end of 21st century (2081–2100); (c) JJA in middle of the 21st century (2041–2060); (d) JJA at the end of 21st century (2081–2100).

5.0°C, respectively.

Figure 5 presents the regional mean temporal evolution of DJF, JJA and annual mean temperature changes (anomalies) over China during 1981–2100 (relative to 1981–2000). As seen in the figure, despite differences in spatial pattern, regional mean changes are similar. Warming trends during 2021–2100 for DJF, JJA, and annual mean are 0.61°C, 0.51°C and 0.53°C per decade, respectively.

Most global models tend to simulate greater warming in winter compared to summer over China [7,9]. Observational studies also report greater warming during cold seasons [32] in recent decades. However, a warming of similar magnitude is simulated in DJF, JJA and annual mean here, as well as in another RegCM3 simulation but driven by a different general circulation model [31]. Further investigation is needed to better understand the mechanisms involved. The simulated warming speed is greater than most AOGCMs [33]. This is mostly because of the greater climate sensitivity of the driving MIROC3.2_hires, as compared to other CMIP3 models [34].

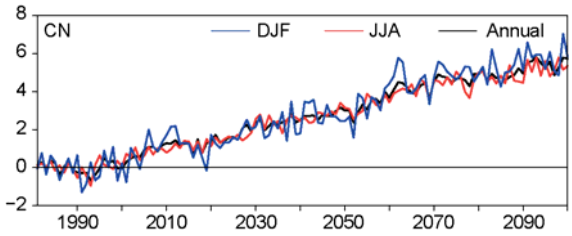

Figure 5 Regional mean temperature change (anomalies) from 1981 to 2100 over China (relative to 1981–2000; °C). Blue: DJF; red: JJA; black: annual mean.

3.2 Precipitation

Figure 6 shows the percent change in DJF and JJA during the middle and end of the 21st century, simulated by RegCM3. As shown in Figure 6(a), in DJF during mid century, there is a general increase, exceeding 10% over most areas. An increase up to 25% is found in parts of Northeast, Northwest, and North China. Precipitation reductions from 10% to 50% dominate the Tibetan Plateau, and these are also found in Western Yunnan Province and part of the Sichuan Basin. The change pattern at the end of the 21st century (Figure 6(b)) shows agreement with that in the middle. However, the increase in North China tends to be greater, and a broader area of decreased precipitation is evident south of the Yangtze River. Regional mean precipitation changes in the middle and end of the century in DJF are 11.3% and 8.4%, respectively.

The pattern of precipitation change in JJA in mid century (Figure 6(c)) shows a similar dipole structure as in DJF over western China, characterized by an increase over the Northwest and decrease over the Tibetan Plateau. A see-saw pattern of changes is found in eastern China, from the

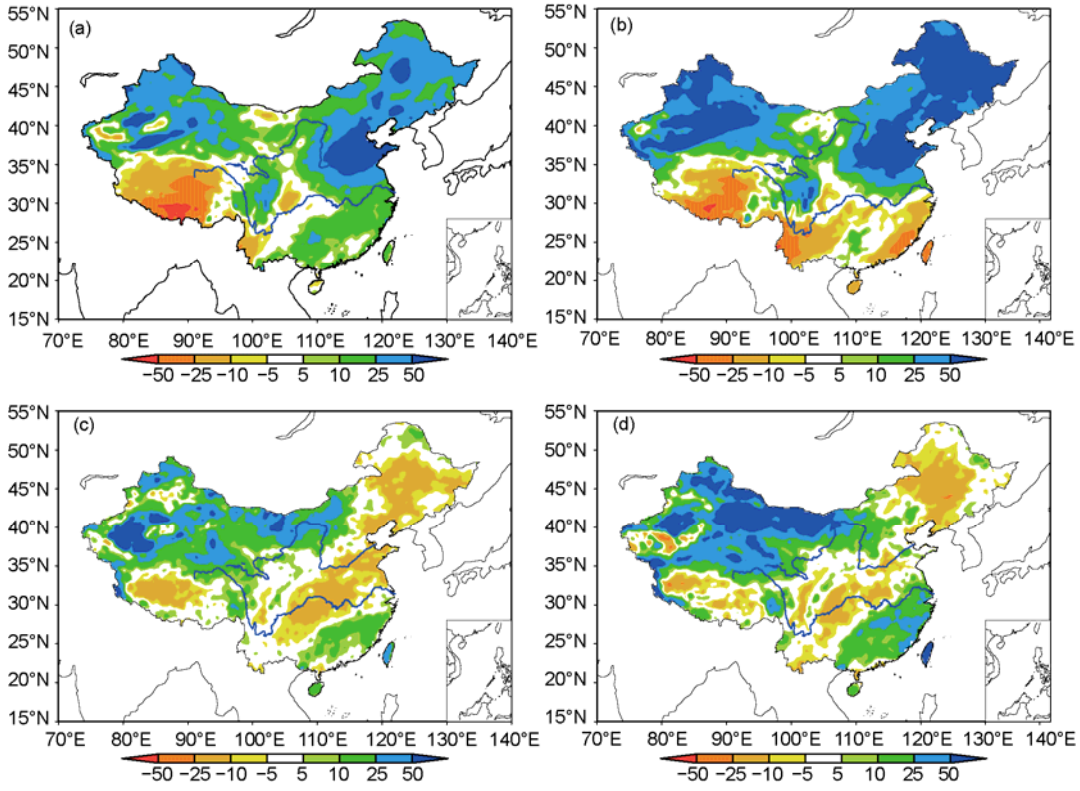

Figure 6 Same as in Figure 4, but for precipitation (%).

Northeast toward the southern coasts. The precipitation change patterns at the end of the century resemble those in the middle, but with larger increases over the region (Figure 6(d)). The simulation produces a slight increase (0.59%) of regional mean precipitation in mid century, and a 4.3% increase at the end.

Figure 7 presents the regional mean temporal evolution of DJF, JJA and annual mean precipitation changes during 1981–2100, relative to 1981–2000. Large interannual variability is shown in the figure, especially for DJF. The linear trends of the changes during 2021–2100 are 0.61%, 0.71% and 1.32% per decade for DJF, JJA, and annual mean, respectively.

3.3 Comparison with a different RegCM3 simulation

A high-resolution climate change simulation has been done previously with RegCM3, but driven by a different global model-FvGCM/CCM3 [31]. This RegCM3 variation used a similar resolution and model domain, but a different emission scenario (A2) with greater greenhouse gas concentrations. However, the two simulations can be roughly compared to each other, because of the greater climate sensitivity of the driving MIROC3.2_hires [34]. The common periods 1961–1990 for present day, and 2071–2100 for the future, were selected for the intercomparison. We focus on precipitation changes only. Inter-model agreement between simulations of driving GCMs and of the nested RegCM3s are shown in Figure 8.

From the figure, the two GCMs projected the same precipitation increase at mid and high latitudes in DJF, which agrees with a projected increase of intense snowfall [35]. A similar precipitation increase is found at mid and high latitudes in the multi-CMIP3 model mean analysis, although a decrease is found at low latitudes [11]. The two GCMs agree on precipitation increases in JJA and in the annual mean, which is also consistent with the multi-CMIP3 model mean [11]. Comparing Figure 8(a) and (b), we see that the agreement of the two RegCM3 simulations is generally similar to that of the driving GCMs, except for the decrease over the Tibetan Plateau. In JJA, the RegCM3 simulations are consistent with an increase in Northwest China, and a decrease over the Tibetan Plateau and Southwest China. However, there is little agreement on the change over Eastern China, where a monsoon climate dominates. The two simulations project opposing change patterns over this area, mostly because of stronger topographic forcings in the RegCM3, which amplify slight differences in the GCM circulation changes, generating large uncertainty in projecting precipitation change in JJA over eastern China (further analysis will be presented in a separate paper). However, as shown in Figure 8(f), there is generally good agreement in the annual mean changes, characterized by a consistent decrease over the Tibetan Plateau and in Southwest China, and an increase in most other locations.

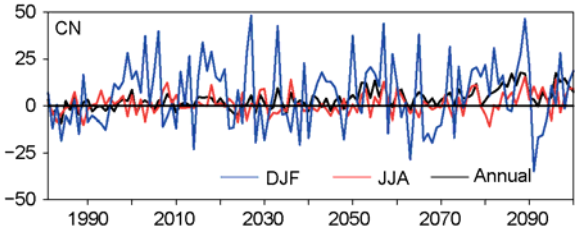

Figure 7 Same as in Figure 5, but for precipitation (%).

4 Discussion and conclusion

A 150-year transient climate change simulation, from 1951–2100, was conducted over East Asia using the regional climate model RegCM3 at 25 km grid spacing. The model was driven by the MIROC3.2_hires GCM, under the IPCC SRES A1B scenario. Our focus was on the simulation of temperature and precipitation and their changes during DJF and JJA. We first evaluated the performance of the RegCM3 model by comparing its simulation against observations. We found that RegCM3 can reasonably reproduce mean surface air temperature and precipitation in DJF and JJA over China, especially so for monsoon precipitation in JJA. We then analyzed the simulated future changes over China, finding:

(1) Substantial warming in both DJF and JJA were simulated over the region. The warming becomes more significant with time during the 21st century. A greater warming in DJF was simulated over the Tibetan Plateau. In JJA, areas with greater warming extend from North China to the Northeast. Similar warming patterns in DJF and JJA were found in both the middle and end of the century.

(2) Regional mean precipitation changes show a slight increase in both DJF and JJA. The spatial distribution of the changes in the middle and end of the 21st century are generally consistent over the region, for both seasons. In DJF, increased precipitation was found in northern areas (North, Northeast and Northwest China), and a decrease over the Tibetan Plateau and southern China. A similar change pattern was evidenced across western China in JJA and DJF. A see-saw change pattern was produced across eastern China.

(3) Comparison was made to a previous RegCM3 simulation, driven by a different GCM. Although the two GCMs show generally consistent precipitation changes over China, the RegCM3 simulations showed differences from the GCMs, in both DJF and JJA. Furthermore, poor agreement was found in the RegCM3 simulation in JJA over eastern China, demonstrating large uncertainties in projecting future precipitation changes. Multi-model ensembles of climate change simulations represent important methods [36]. They should be further conducted for better understanding and reduction of these uncertainties, and for achieving more

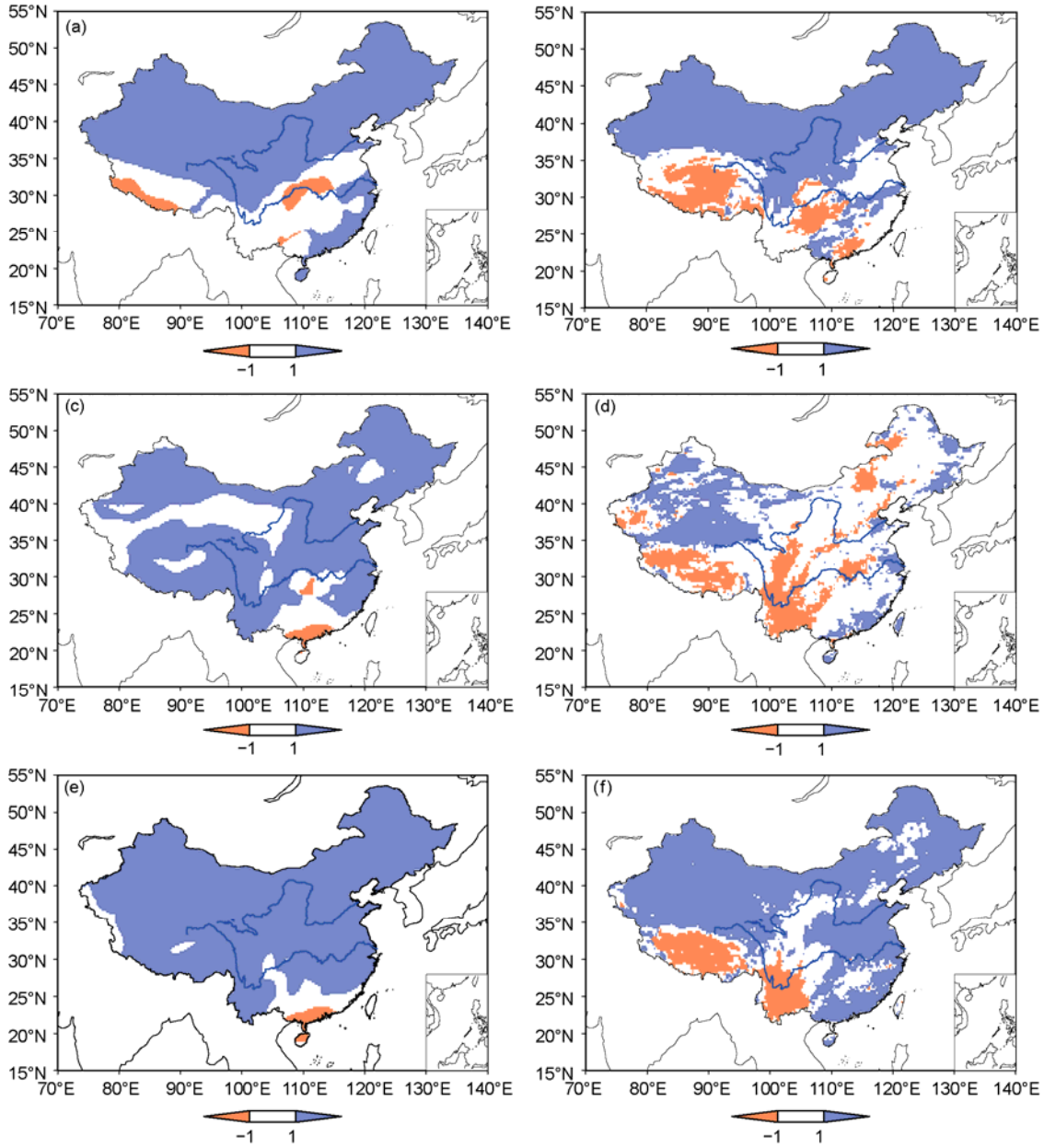

Figure 8 Agreement in the sign of projected precipitation change between the GCMs and driving RegCM3 simulations (blue/red indicates that both models simulate an/a increase/decrease). (a) GCMs in DJF; (b) RegCM3 in DJF; (c) GCMs in JJA; (d) RegCM3 in JJA; (e) GCMs in annual mean; (f) RegCM3 in annual mean.

scientifically robust and valuable conclusions in the projection of future regional climate change.

Because of the limited scope of this paper, we focused only on mean temperature and precipitation in DJF and JJA. Future work will include in-depth analysis of the model results; for example, changes in variability and extremes, as well as comparison of the RegCM3 simulations with the driving MIROC3.2_hires. Finally, data are available for impact studies that address 21st-century climate change impacts on agriculture, water resources, ecosystems, and other sectors in China.

This work was supported by the National Basic Research Program of China (2009CB421407), China-UK-Swiss Adapting to Climate Change in China Project (ACCC), and the Special Research Program for Public-welfare Forestry (200804001). The authors would like to thank the modeling group of MIROC3.2_hires in preparing and providing the data to drive RegCM3 (Dr. Seita Emori, Dr. Manabu Abe, and others).

1 IPCC. Climate Change 2007: The Physical Science Basis. In: Solomon S, Qin D, Manning M, et al., eds. Contribution of Working Group 1 to the Fourth Assessment Report of the Intergovernmental Panel on Climate Change. Cambridge, United Kingdom and New York: Cambridge University Press, 2007. 1–18

2 Giorgi F. Simulation of regional climate using a limited area model nested in a general circulation model. J Clim, 1990, 3: 941–964

3 Christensen J H, Hewitson B, Busuioc A, et al. Regional Climate Projections. In: Solomon S, Qin D, Manning M, et al., eds. Climate Change 2007: The Physical Science Basis. Contribution of Working Group 1 to the Fourth Assessment Report of the Intergovernmental Panel on Climate Change. Cambridge, United Kingdom and New York: Cambridge University Press, 2007. 847–940
4 Hirakuchi H, Giorgi F. Multiyear present-day and 2xCO_2 simulations of monsoon climate over eastern Asia and Japan with a regional climate model nested in a general circulation model. J Geophys Res, 1995, 100: 21105–21125
5 Gao X J, Zhao Z C, Ding Y H, et al. Climate change due to greenhouse effects in China as simulated by a regional climate model. Adv Atmos Sci, 2001, 18: 1224–1230
6 Gao X J, Shi Y, Song R Y, et al. Reduction of future monsoon precipitation over China: Comparison between a high resolution RCM simulation and the driving GCM. Meteorol Atmos Phys, 2008, 100: 73–86
7 Jiang D B, Wang H J, Lang X M. Multimodel ensemble prediction for climate change trend of China under SRES A2 scenario (in Chinese). Chin J Geophys, 2004, 47: 776–784
8 Gao X J, Pal J S, Giorgi F. Projected changes in mean and extreme precipitation over the Mediterranean region from a high resolution double nested RCM simulation. Geophys Res Lett, 2006, 33: L03706
9 Zhou T J, Yu R C. Twentieth century surface air temperature over China and the globe simulated by coupled climate models. J Clim, 2006, 19: 5843–5858
10 Ju L X, Wang H J, Jiang D B. Simulation of the Last Glacial Maximum climate over East Asia with a regional climate model nested in a general circulation model. Palaeogeogr Palaeoclimatol Palaeoecol, 2007, 248: 376–390
11 Xu Y, Gao X J, Giorgi F, et al. Upgrades to the REA method for producing probabilistic climate change predictions. Clim Res, 2010, 41: 61–81
12 Yu E T, Wang H J, Sun J Q. A quick report on a dynamical downscaling simulation over china using the nested model. Atmos Oceanic Sci Lett, 2010, 3: 325–329
13 Wang H J, Yu E T, Yang S. An exceptionally heavy snowfall in Northeast China: Large-scale circulation anomalies and hindcast of the NCAR WRF model. Meteorol Atmos Phys, 2011, 113: 11–25
14 Giorgi F, Marinucci M R, Bates G T. Development of a second-generation regional climate model (RegCM2). Part I: Boundary-layer and radiative transfer processes. Mon Weather Rev, 1993, 121: 2794–2813
15 Giorgi F, Marinucci M R, Bates G T, et al. Development of a second-generation regional climate model (RegCM2). Part II: Convective processes and assimilation of lateral boundary conditions. Mon Weather Rev, 1993, 121: 2814–2832
16 Pal J S, Giorgi F, Bi X Q, et al. The ICTP RegCM3 and RegCNET: Regional climate modeling for the developing world. Bull Amer Meteorol Soc, 2007, 88: 1395–1409
17 Kiehl J, Hack J, Bonan G, et al. Description of the NCAR Community Climate Model (CCM3). NCAR Technical Note, NCAR/TN-420 STR. 1996
18 Zeng X, Zhao M, Dickinson R E. Intercomparison of bulk aerodynamic algoriths for the computation of sea surface fluxes using toga coare and tao data. J Clim, 1998, 11: 2628–2644
19 Holtslag A, de Bruijin E, Pan H L. A high resolution air mass transformation model for short-range weather forecasting. Mon Weather Rev, 1990, 118: 1561–1575
20 Pal J S, Small E E, Eltahir E. Simulation of regional-scale water and energy budgets: Representation of subgrid cloud and precipitation processes within RegCM. J Geophys Res, 2000, 105: 29579–29594
21 Grell G. Prognostic evaluation of assumptions used by cumulus parameterizations. Mon Weather Rev, 1993, 121: 764–787
22 Fritsch J M, Chappell C F. Numerical prediction of convectively driven mesoscale pressure systems. Part I. Convective parameterization. J Atmos Sci, 1980, 37: 1722–1733
23 Dickinson R E, Kennedy P J, Henderson-Sellers A, et al. Biosphere-atmosphere transfer scheme (bats) for the ncar community climate model. Technical Report of National Center for Atmospheric Research. 1986
24 Liu J Y, Liu M L, Zhuang D F, et al. Study on spatial pattern of land-use change in China during 1995–2000. Sci China Ser D-Earth Sci, 2003, 46: 373–384
25 K-1 Model Developers. K-1 coupled model (MIROC) description. K-1 technical report 1. In: Hasumi H, Emori S, eds. Tokyo: Center for Climate System Research, University of Tokyo. 2004
26 Lucarini V, Calmanti S, Dell'Aquila S, et al. Intercomparison of the northern hemisphere winter mid-latitude atmospheric variability of the IPCC models. Clim Dyn, 2007, 28: 829–848
27 Xu C H, Shen X Y, Xu Y. An analysis of climate change in East Asia by using the IPCC AR4 simulations (in Chinese). Adv Clim Changes Res, 2007, 3: 287–292
28 Xu Y, Gao X J, Shen Y, et al. A daily temperature dataset over China and its application in validating a RCM simulation. Adv Atmos Sci, 2009, 26: 763–772
29 Xie P P, Yatagai A, Chen M Y, et al. A gauge-based analysis of daily precipitation over East Asia. J Hydrol, 2007, 8: 607–626
30 Zhang D F, Gao X J, Ouyang L C, et al. Simulation of present climate over East Asia by a regional climate model. J Trop Meteorol, 2008, 14: 19–23
31 Gao X J, Shi Y, Giogi F. A high resolution simulation of climate change over China. Sci China Ser D-Earth Sci, 2011, 54: 462–472
32 Tang H Y, Zhai P M. Comparison of variations of surface air temperatures in eastern and western China during 1951–2002 (in Chinese). Chin J Geophys, 2005, 48: 526–534
33 Jiang D B, Zhang Y, Sun J Q. Ensemble projection of 1–3°C warming in China. Chin Sci Bull, 2009, 54: 3326–3334
34 Randall D A, Wood R A, Bony S, et al. Climate models and their evaluation. In: Solomon S, Qin D, Manning M, et al., eds. Climate Change 2007: The Physical Science Basis. Contribution of Working Group 1 to the Fourth Assessment Report of the Intergovernmental Panel on Climate Change. Cambridge, United Kingdom and New York: Cambridge University Press, 2007. 589–662
35 Sun J Q, Wang H J, Yuan W. Spatial-temporal features of intense snowfall events in China. J Geophys Res, 2010, 115: D16110
36 Giorgi F, Jones C, Asrar G, et al. Addressing climate information needs at the regional level: the CORDEX framework. WMO Bull, 2009, 58: 175–183